# The decline of Fraxinus angustifolia Vahl in a Mediterranean salt meadow: Chlorophyll fluorescence measurements in long-term field experiment

Jean-Philippe Mevy, Frédéric Guibal, Caroline Lecareux, Franco Miglietta

# The decline of *Fraxinus angustifolia* Vahl in a Mediterranean salt meadow: Chlorophyll fluorescence measurements in long-term field experiment.

**J.P. Mevy[1*], F. Guibal[1], C. Lecareux[1] and F. Miglietta[2,3].**

1 Aix-Marseille University, Avignon University, CNRS, IRD, IMBE, Marseille, France

2 Institute of Biometeorology, National Research Council (CNR- IBIMET), Via Caproni 8, 50145 Firenze, Italy

3 IMèRA, Institut d'Etudes Avancées de l'Université Aix-Marseille, 2 Place Le Verrier, 13004 Marseille, France

Author for correspondence:

Jean-Philippe Mevy

Tel : +33 0413550766

Email ; jean-philippe.mevy@imbe.fr

## Abstract:

The ecological transition zones also known as ecotones are specific ecosystems but how global change will affect their biodiversity and functioning is poorly understood. In the case of the areas at the interface between riparian forest and salt meadows the biodiversity conservation remains a major issue. The aim of this work was to evaluate the effects of a salty environment on *Fraxinus angustifolia* a non-halophyte species. For this, the photochemistry of PSII was *in situ* explored during the summer between 2007 and 2016. The predawn maximum quantum efficiency of PSII (Fv/Fm) was always greater than 0.8 which indicates an absence of chronic photoinhibition induced by salinity. During these years, the light kinetic of the actual quantum yield of PSII ($\Phi_{PSII}$) was studied. It appears that this yield is generally higher in salty environments than in the riparian forest. Multivariate analysis, showed that the dissipation regulated light energy faction ($\Phi_{NPQ}$), the photochemical quenching (qP) and the Fd/Fs ratio constitute the main explanatory variables of $\Phi_{PSII}$ changes. The subsequent two-way-ANCOVA carried out demonstrated that $\Phi_{NPQ}$ was weaker in saline environments, suggesting a better efficiency of photosystem collecting antennas. Meanwhile, the analysis of photosynthetic pigments did not exhibited a salt effect except the significant accumulation of chlorophyll a in 2016. In order to address the question of the salt-related toxicity, sodium ion contents in the leaves were found to be identical in the two sites, suggesting the establishment of an energy-dependent mechanism of salt exclusion/retention in roots. The growth rings of *F.angustifolia* in saline areas highly follows the annual water deficit changes. Between 2007 and 2016, the biomass in the salt meadow was higher with a peak in 2011 representing 60% of the biomass of control individuals. But, since 2011 a

continuous decline of growth was recorded. Water conditions seem to constitute a limiting factor even if the photosynthetic apparatus generates the excess metabolic energy necessary to cope with the saline toxicity. This study thus highlighted the plasticity of the photochemistry of the PSII depending to the environmental conditions of the salt meadows. It also shows the vulnerability of an ecotone through the decline in the productivity of a glycophyte with climate change. This augurs for changes in the composition of plant communities which is in favor of strict halophytes.

**Key words:** *Fraxinus angustifolia*; salt stress; PSII photochemistry; salt meadow; water deficit; ecophysiology.

## 1. Introduction

Global change projections of wetland ecosystems such as salt marshes include sea-level rise and extreme climatic events (Thorne et al., 2012). Salt meadows spread over narrow transitional areas between sea and terrestrial environments which are considered as high-risk zones subject to climate change impacts (Thorne et al., 2012). In these ecosystems, several taxonomic groups of plants coexist with salt requirements which are highly contrasted. They are divided into euhalophytes and facultative halophytes but typically an halophyte is defined as a plant that grows in soil conditions of more than 200 mM NaCl concentration (Flowers and Colmer, 2008) . Besides salinity conditions, biotic factors such as competition between individuals are also to be considered in terms of saltmarshes functioning (Pennings et al., 2005). Overall, it appears that the hydro-period regime that depends on specific precipitation and evaporation conditions is one of the main factors regulating the creation of niches for wetland plant species (Foti et al., 2012).

The question of the spatial distribution of species between the seashore and the boundary of non-halophytic terrestrial vegetation has been addressed by several authors (Pennings et al., 2005; Silvestri et al., 2005). For instance taking into account the elevation gradient, four clusters reflecting the composition of plant community were shown (Bang et al., 2018). However, the scarcity of studies focussing on the salt marsh-terrestrial boundaries was underlined (Traut, 2005; Veldkornet et al., 2015). Indeed, the border between the salt marsh and the adjacent upland (terrestrial vegetation) occupies a narrow surface also recognized as ecotone. These habitats are submitted to particular abiotic conditions leading to a plant community assembly that is specific to one or both of the adjacent ecosystems. In the Mediterranean region and in the Bouches-du-Rhône in particular, salt meadows develop at the

confluence of rivers and the Etang de Berre. This is the case for the river Arc which exhibits a steep fall of the presence of trees from the riparian forest in the upland. Among the riparian woody species only few specimens of *Fraxinus angustifolia* Vahl (narrow-leaved ash) were observed in the salt marsh upland transition zone possibly in the area so-called ecotone. Hence, information on species with narrow biotope tolerance might best characterize the effects of climate change (James and Zedler, 2000).

*F. angustifolia* belongs to the family Oleaceae and is widespread across Southern Europe. In Mediterranean basin the plant is often encountered in riparian corridors. In Croatia for example, narrow-leaved ash is considered as one of the most important tree species of lowland floodplain forests and its sensitivity to drought was shown (Drvodelic et al., 2016). But, how *F. angustifolia* will cope with salinity and drought expected with climate change is poorly explored. More generally exploring the mechanisms of glycophytes adaptation to salinity is becoming a great challenge because soil salinization is recognized as a global problem resulting in soil degradation, arable land surface decrease and ecological environmental disturbance (Hu et al., 2019). By comparing two *Solanum* species, one glycophyte and the other salt-tolerant, it has been shown that ethylene induction plays a key role in salinity tolerance through an improved stomatal conductance, an efficient osmotic adjustment and the increase of $Na^+$ accumulation in shoots (Gharbi et al., 2017). In roots of the glycophyte *Arabidopsis thaliana* (L.) Heynh., salt stress triggered principally defence proteins as those involved in ROS scavenging whereas for the xero-halophyte *Zygophyllum xanthoxylum* Engl. Ex Dippel, $Na^+$ uptake was improved in addition with metabolic shifts towards *de novo* synthesis of glucose in order to sustain growth (Chai et al., 2019). Similarly, retention of sodium cations in roots thus preventing their translocation to shoots is considered as a key adaptive mechanism of glycophytes to salt stress (Assaha et al., 2017; Hasegawa, 2013). Root sequestration of sodium cations not only improves the water balance by adequate osmotic adjustment but also preserves the photosynthetic machinery from ionic toxicity. Thus, from the xero-halophyte *Nitraria retusa* (Forssk.) Asch., PSII photochemistry and carotenoid content were not affected by salinity whereas a significant reduction in pigment concentrations and chlorophyll fluorescence parameters were observed from the glycophyte *Medicago arborea* L. (Boughalleb et al., 2009). This led to suggest that the decrease of the photosynthetic activity is likely the result of damages in the photosynthetic apparatus rather than factors driving stomatal closure. Other authors have also shown that the maximum quantum efficiency of PSII is highly reduced for rice salt-sensitive cultivars consecutively to

salt stress application as compared to salt-tolerant cultivars. Similarly, the minimum fluorescence intensity (F0), the actual quantum efficiency (PSII) and the None-Photochemical Quenching (NPQ) were identified as the main fluorescence parameters that change depending on the intensity of salt stress (Tsai et al., 2019). Besides the ionic toxicity induced by soil salinity, water availability also constitutes a major constraint for glycophytes survival in saltmarshes. Although, chlorophyll a fluorescence has been used as a signal for monitoring plants response to drought in several reports (Dalberto et al., 2017; Vaz et al., 2016; Wang et al., 2016) few works deal with both drought and salinity effects. Moreover, plant *in situ* often experience multifactorial stress conditions.

Understanding how a glycophyte may stabilize its photosynthesis activity also maintaining its ionic homeostasis under high soil salinity can help provide insight in terms of plant breeding and ecological management. In this report we evaluate the ecological fitness of a glycophyte *F. angustifolia* native to the saltmarsh/upland transition zone also termed ecotone upon a highly sensitive to global climatic change variables. Second, we hypothesized that the predicted increase warming and summer drought in Mediterranean basin would lead to more NaCl accumulation requiring additional metabolic energy to sustain growth and defence molecules biosynthesis. Finally we considered that the global change would drive profound changes in the assemblages of plant communities into the ecotones of the deltaic zones of the Mediterranean rivers.

## 2. Material and methods

### *2.1 The study site*

The area that was the subject of this study is located in the Arc delta ecotone and in the riparian forest of the same river (Berre-l'Etang, France). The Arc delta occupies an area of 190 ha. It is associated with hydromorphic soils covered with a halophilic vegetation, which extend about 700 m wide. Upstream the deltaic zone (1.4 km), the riparian forest is mainly constituted by ash, poplar and white willow. The ecotone was characterized by the occurrence of both euhalophytes and facultative halophytes as well as some specimens of *Fraxinus angustifolia*, namely: *Sueda vera* Forssk. ex J.F.Gmel., *Limonium narbonense* Mill., *Limonium cuspidatum* (Delort) Erben, *Chenopodium chenopodioides* (L.) Aellen, *Tamarix gallica* L., *Obione portulacoides* (=Atriplex portulacoides L.) and *Plantago coronopus* L. The meteorological data were obtained from the nearest station namely Marignane which is

located at about 11 km away as the crow flies. Five to six trees (*F. angustifolia*) of similar height and diameter were chosen in each zone during this study.

*2.2 Modulated chlorophyll fluorescence parameters monitoring*

Fluorescence data were obtained using Hansatech fluorometer (FMS2). Leaves (3 per tree) were dark-adapted for 30 min using the dark-adaptation clip prior to the application of a low pulsed amber light intensity to determine the minimum fluorescence ($F_0$) followed by the application of a saturating pulse for the maximum fluorescence measurement ($F_m$) such that all primary quinone electron acceptors in PSII are closed ($Q_A$ fully reduced). These data allow to calculate the maximum quantum efficiency through the ratio $F_v/F_m$ where $F_v$ ($F_m$-$F_0$) corresponds to the variable fluorescence. This ratio was determined at predawn, dawn and in diurnal period.

The diurnal course of chlorophyll parameters was monitored on 28$^{th}$ august 2007 from 9:00 h to 18:00 h by using successively the dark adaptation clip and the PAR/temperature leaf-clip which is designed for measurements under ambient light conditions**.** Thus additional variables were recorded from light acclimated leaves: minimum ($F'_0$) maximum ($F'_m$) and the steady state ($F_s$) values of fluorescence. Through these data as well as $F_m$ and $F_0$ the following fluorescence parameters were determined: The photochemical efficiency in the light adapted state of photosystem II ($\Phi_{PSII}$) calculated as ($F'_m$- $F_s$)/$F'_m$ according to Genty et al. (1989), the non-photochemical quenching coefficient of chlorophyll fluorescence (NPQ), calculated as ($F_m$ – $F'_m$)/$F'_m$ (Bilger and Björkman, 1990) which expresses the dissipation of excess energy as heat and the photochemical quenching (qP*)*coefficient, which was calculated from ($F'_m$ - $F_s$)/($F'_m$- $F'_0$) that gives an indication of the proportion of PSII reaction centers that are open (Maxwell and Johnson, 2000). An alternative non-photochemical quenching coefficient, QNP =(Fm-F'm/Fm-$F_0$) was also determined (Schreiber et al., 1986).

Light response kinetic measurements were carried out at dawn by selecting four incident photosynthetically active irradiance (PAR) intensities in order to simulate the half diurnal light radiation change: 300, 600, 900 and 1200 µmol Photons $m^{-2}s^{-1}$. The light saturating pulse (8.000 µmol Photons $m^{-2}s^{-1}$) was applied for each PAR intensity only when the steady-state fluorescence intensity ($F_s$) was reached. This was checked prior to the design of a specific light kinetic script. In addition to the above-mentioned fluorescence parameters, other parameters were calculated for each actinic light application: the quantum efficiency of regulated ΔpH and/or xanthophyll-dependent non-photochemical dissipation processes in the

antenna of PSII ($\Phi_{NPQ}$= Fs/F'm – Fs/Fm). The quantum efficiency of the constitutive non-photochemical fluorescence and energy dissipation ($\Phi_{f,D}$=Fs/Fm) according to Hendrickson et al. (2005). The Chlorophyll fluorescence decrease ratio was calculated as: Fd/Fs= Fm-Fs/Fs (Lichtenthaler et al., 2005). Also, the rate of the linear electron transport was determined:

ETR = 0.5xPARx0.87x $\Phi_{PSII}$ assuming that the photon flux are equally distributed between the two photosystems.

*2.3 Simultaneous gas exchange and fluorescence monitoring*

The leaf gas exchange and fluorescence parameters were simultaneously determined using a gas exchange system (LI-6400XT; LI-COR Inc., Lincoln, NE, USA) equipped with a fluorescence chamber head. $CO_2$ assimilation rate (*A*), internal $CO_2$ (*C*i) and stomatal conductance ($g_s$) were determined. All the measurements were carried out at 25°C and the relative humidity of the chamber was set at 70%, while the amount of blue light was set to 10% of the photosynthetic photon flux density for optimized stomatal aperture. In light-adapted leaves, the steady state fluorescence yield (*F*s) was recorded and the maximum fluorescence (*F'*m) obtained after application of a saturating white light pulse (8.000 μmol photons $m^{-2}$ $s^{-1}$, 0.8 s). The actinic light was then turned off and far-red illumination was applied (2 μmol photons $m^{-2}$ $s^{-1}$) to measure the light-adapted minimum fluorescence (*F'*0). Using these parameters, $\Phi_{PSII}$, qP and the ratio F'v/F'm = (F'm-F'o)/F'm which corresponds to the efficiency of the energy harvesting by the oxidized PSII reaction centers in light condition were determined.

*2.4 Predawn leaf water potential determination*

Water potential (Ψ) was measured using a pressure chamber of Scholander type (Scholander et al., 1965), from mature fully expanded leaves of randomly selected plants. The measurements were carried out from five trees per site at 05:00 h then finished before sunrise.

*2.5 Soil and leaf sodium ions concentration*

Five trees and five soil samples were considered for each condition: salt meadow and the control. Plant samples was composed by a pool of five leaves per tree. Soil and leaf samples were ash transformed in a muffle furnace. The extracted solutions were analysed for $Na^+$ concentrations by using an Ion Chromatograph (Dionex Model DX 120, USA). The column

used was a CS16 with hydroxymethanesulfonic acid (26 mM) as eluent which a flow rate set at 1ml/min. Electrical conductivity was the mode of cations detection.

*2.6 Photosynthetic pigments analysis*

Leaves (a pool of five leaves per tree from five trees in each site) were collected at predawn then wrapped in aluminum foil to avoid for degradation of pigments by light and finally stored at – 20°C until analysis in the laboratory. Chlorophylls and total carotenoids were extracted with acetone (80%) and filtered through Millipore membrane (0.2 µm pore size). Quantification was performed with a spectrophotometer (BioMate$^{TM}$3) by measuring their absorbance at 663, 646 and 470 nm (Lichtenthaler and Wellburn, 1983).

*2.7 Dendrochronology*

The sampling process took place during the spring 2017. We selected six dominant and mature ashes separated by at least 8 m from each other in the salt meadow; six other dominant ashes were selected as control trees. One core per tree at 1.3 m height was collected with a Swedish increment borer. In the laboratory, cores were prepared according to standard dendrochronological procedures (Fritts 1976). All cores were air-dried, glued onto groove boards, sanded with progressively finer grade sandpaper to produce smoothed surfaces on which the tree-ring boundaries were clearly visible and visually crossdated under a binocular to ensure that each ring was dated to the correct calendar year. Then, ring-width series were measured to the nearest 1/100 mm using a LINTAB6 measuring table (Rinntech®) and the TSAP-Win software (Rinn 2003). All ring-width series were crossdated graphically and crossdating was checked using the COFECHA software (Holmes, 1983) by assessing the consistency of the different ring-width series among trees.

*2.8 Statistical analysis*

A Student test was performed to compare the two sites for each interval of time regarding to the diurnal measurements of fluorescence parameters.

For the predawn physiological indicators ($F_v/F_m$, pigment content and $\Psi$) a two-way ANOVA was designed to assess the relationship between the two independent variables (Site x Year) on each dependent variable followed by Tukey's HSD (Honestly Significant Differences)

tests. The PSII photochemistry parameters obtained from light kinetics were first treated by a multivariate analysis in order to determine the main explicative fluorescence parameters of the actual quantum yield kinetics. This was performed using R statistical software (R development Core Team, 2009) and the package "FactoMineR" Thus, covariance analyses (ANCOVA), with light intensities fixed as covariate were used to examine the effect of site and year on the pertinent explicative fluorescence variables. Curves fitting and statistical analyses were performed using Statgraphics Centurion XV software and R statistical software.

## 3. Results

### *3.1 Annual changes in climatic conditions of the study site*

The study area was located near the village of Mauran at 11 km of the nearest meteorogical station which is that of Marignane (France). As shown in table 1, during this last decade, summer air temperature varied from 23 to 25°C. There was no significant difference between the years (one-way-ANOVA, $F$=2.12, $P$=0.065). However, the cumulated precipitation varied considerably (10-139 mm) resulting in similar changes in soil water deficit. For instance the highest water deficit was recorded in 2016 (-659 mm) while the lowest one was observed in 2011 (-4.18 mm).

### *3.2 Interannual radial growth*

Analyzes of the cores collected from the individuals located at the two study sites allowed us to address their radial growth over the last ten years. The results clearly show that *F. angustifolia* grows better in salt meadows than the control site (Fig. 1). A peak of radial growth was recorded in 2014, where growth in the saline area was twice that of the riparian bank. However, since 2011, this growth has been falling to equal the radial growth of individuals in the control habitat.

### *3.3 Leaf water and sodium ion status*

*F. angustifolia* environmental conditions in both salt meadow and riparian forest bank were first characterized at the beginning of august 2007. Soil water availability was characterized by the measurement of leaf water potential in the absence of any transpiration flux as well as leaves and soil sodium chloride contents. Predawn water potential was higher in control stand

compared to salt marsh individuals. Leaves $Na^+$ content were similar while soil $Na^+$ content in salt meadow site was about 13-fold that of the riparian forest bank (Table 2).

*3.4 The diurnal variation of chlorophyll fluorescence parameters*

From 9:00 h to 18:00 h several chlorophyll fluorescence data were recorded (Fig. 2). The maximum quantum efficiency of PSII (Fv/Fm) was significantly higher for samples of salt meadow site compared to those of the riparian forest only from 9:00 h to 13:00 h. For instance, at 13:00 h the ratios Fv/Fm were 0.739 and 0.614, respectively (Fig. 2A). When leaves were light acclimated, the actual efficiency of PSII photochemistry ($\Phi_{PSII}$) decreases by late morning to 16:00 h then rises until 6:00 h pm in both cases (Fig. 2B). However at 9:00h $\Phi_{PSII}$ of *F. angustifolia* located in salty soils was about 2-fold that of none salty grown specimens. The exitonic energy used for the reduction of the plastoquinone pool, determined by the photochemical quenching coefficient (qP) exhibited similar patterns for both sites but with a significant difference obtained also only at 9:00 h am (Fig. 2C). Alternatively, the excess of absorbed excitation energy may be dissipated through non-photochemichal processes referred as NPQ. No significant difference was found between the two sites in the morning (Fig. 2D).

Hence, it seems that *F. angustifolia* quantum yield in salty soil condition is higher than the control during the morning and this may be explained by both photochemical quenching mechanisms and PSII antenna efficiency. This led to further investigation regarding to the predawn maximum quantum efficiency and the plant response to light kinetic taking into account the interannual variability.

*3.5 Predawn Fv/Fm and steady-state light response of chlorophyll fluorescence parameters in field conditions*

*3.5.1 Predawn Fv/Fm*

The analysis of the maximum quantum efficiency carried out between 2007 and 2016 showed that the factors site and year interact together ($F$=5.31; $p$<0.001). Hence, the predawn ratios Fv/Fm of the sites were compared year by year. As a result (Fig. 3) *F. angustifolia* exhibited significant differences between sites in 2009 and 2016. For the former date, a lower ratio was obtained in salt meadow compare to the control; 0.819 and 0.886, respectively. For the latter,

an opposite response was shown because salt meadow Fv/Fm was about 0.05 units higher than the data recorded from control samples. The predawn ratio was also tested site by site for all the years which revealed that the ratio Fv/Fm tends to be lower in control with greater variability throughout the years (Fig. 4).

*3.5.2 Dawn light kinetic fluorescence parameters measurements*

Solar course during half a day was mimed by the implementation of a script where the intensity of the light increases from 300 to 1200 µmol. photon.$m^{-2}$.$s^{-1}$ in 4 steps. Fluorescence data were recorded during 6 years then first examined through the quantum yield kinetic. Two-way ANCOVA with light intensity as covariate was carried out. A significant effect of the factors year ($F=61.54$ $p<0.001$) and site ($F=9.38$ $p<0.001$) was shown and no interaction was found between them. Thus, the site effect on the dependent variable $\Phi_{PSII}$ was tested year by year. As a result, the photochemical quantum yield decreases exponentially with light intensity (Fig. 5) with significant differences between the two sites except in 2014.The photosynthetic performance of individuals in salt meadows was higher than that of the controls. It is thus possible to summarize the functioning of the photosynthetic machinery in 2 types of response. The first one is characterized by large variations in the actual quantum yield at low light intensities as in 2007, 2008 and 2016. The second type of response is manifested by an increasing difference as light intensities increase. This is the case in 2015 and 2009 where the quantum yields were about 0.8. It appears that soil salinity contributes to increase *F. angustifolia* PSII quantum yield through physiological mechanisms that change depending to the year. This arises the question of the identification of the fluorescence parameters that explain these variations of the effective quantum yield. A multivariate analysis was performed in order to prioritize the fluorescence parameters involved. The factor map of the variables denotes a total variance of 89.46 % (Fig.6). Interestingly, $\Phi_{PSII}$ is strongly correlated to axis 1 (correlation coefficient: 0.99) followed by $\Phi_{NPQ}$ (correlation coefficient: 0.96) and qP (correlation coefficient: -0.87). As for axis 2, the main explanatory variable is Fd/Fs (correlation coefficient: 0.87). In summary the variations of $\Phi_{PSII}$ are mainly explained by non-photochemical quenching mechanisms followed by the ratio Fd/Fs. For the former, the two-way ANCOVA performed showed a significant site ($F=11.69$, $p<0.001$) and year ($F=50.35$, $p<0.001$) effects, no interaction was found between the two factors. In these conditions, $\Phi_{NPQ}$ was compared between sites, year by year. The results showed that $\Phi_{NPQ}$ in the salty areas was lower than that of the control except in 2014, 2015 (Fig. 7).

### *3.6 Gas exchange and fluorescence measurements*

Simultaneous measurements of gas exchanges and fluorescence data were carried out in 2009 with a Licor 6400 equipped with the fluorescence chamber. The responses of *F. angustifolia* to salt meadow environmental conditions were examined through the measurements of leaf net photosynthesis (A), leaf internal $CO_2$ concentration (Ci), PSII antenna efficiency (Fv'/Fm'), the photochemical quenching qP and the quantum yield of PSII. As shown in table 3 salt meadow plants exhibited a slight increase of the net photosynthesis (3.17 µmol. $CO_2.m^{-2}.s^{-1}$) compared to the controls (2.93 µmol. $CO_2.m^{-2}.s^{-1}$). Similar result was also obtained for leaf internal $CO_2$ content. However, no differences were found for the quantum yield and related fluorescence data.

### *3.7 Photosynthetic pigments analysis*

The concentrations of chlorophylls and total carotenoids contents were measured from the two sites throughout six years. Based on the data obtained for chlorophyll a there was an interaction between the factors site and year ($F=2.43$; $p<0.05$). Sites were thus compared year by year but no significant difference was found except in 2016 where chlorophyll a contents from salt meadow samples were 3-fold higher compare to the controls (Fig. 8A). For the other pigments no interaction was ascertained between the two factors and significant changes were obtained only over the years. Hence, the highest contents of chlorophyll b were recorded in 2008 whereas the lowest values were obtained in 2007 (Fig. 8B).Total carotenoids concentration (Fig. 8C) in 2008 was about 75 µg/g of DW which represents the highest values recorded during the years investigated while the lowest data were obtained in 2015 (27 µg/g of DW).

## 4. Discussion

In this report we showed for the first time a long term survey of the *in situ* adaptation of a glycophyte to salt march conditions based on chlorophyll fluorescence signals. The model used was *F. angustifolia* which occurs naturally in several Mediterranean deltaic zones unlike to most of riparian forest species.

During the last decade, the tree-rings of individuals growing in the salt marsh showed clearly two effects: on one hand, the biomass is greater than that of the individuals in the control area (Fig. 1) and on the other hand, this biomass varies according to the fluctuations of water deficit (Table 1). In particular, from the peak of 2011 the biomass has steadily decreased to reach that of the control individuals in 2017. A higher biomass could be the result of intense photosynthetic activity at the level of both light and enzymatic reactions but also the fact of a greater availability of nutrients. Indeed, river mouths are recognized as areas with high concentrations of mineral elements because of the importance of alluvial deposits. This is true for halophytes but glycophytes have to cope with salinity: 13-fold higher as found in this study (Table 2) suggesting the need of additional metabolic energy. Thus, the light-dependent reactions of photosynthesis were followed through several parameters based on the fluorescence of chlorophyll a. Measurements of the maximum quantum efficiency before sunrise did not show any particular stress since the values obtained were all greater than 0.75 (Björkman and Demmig, 1987). This also indicates the lack of chronic photoinhibition or salt induced toxicity to PSII (Yan et al., 2015). However, for the year 2016, which was characterized by the greatest water deficit (P=10 mm), the ratio Fv/Fm measured in the saline zone was significantly higher than of the control zone. Similarly, the levels of chlorophyll a were three times higher compared to individuals in the control zone (Fig.7A). This is an unexpected result because the ratio Fv/Fm trends to decrease with stress intensity as well as chlorophyll a contents (Manaa et al., 2019; Masondo et al., 2019). Nevertheless, the increase of chlorophyll a content under salinity was observed from individuals of *Phragmites karka* (Retz.) Trin ex Sternd (Shoukat et al., 2019) as such, the increase of chlorophyll content has been considered to be a marker of resistance to salinity (Acosta-Motos et al., 2017).This would mean that the increase in the Fv/Fm ratio corresponds to an adaptive response of *F. angustifolia* to both drought and salinity. Indeed chlorophyll a is present as a dimer in the reaction center of the photosystems, an increase in its concentration could result in an increase in the number of photosystems and consequently a better photosynthetic capacity of individuals to mitigate the environmental constraints.

Given the absence of chronic photoinhibition, fluorescence measurements were conducted in order to understand the dynamics of photosynthesis light reactions. Initially, the measurements made between 9:00 h and 18:00 h clearly showed that the actual photochemical yield ($\Phi_{PSII}$) of individuals in salty environment was higher than those in the control area (Fig. 2B). Subsequently, kinetics measurements were carried out by simulation of light intensity variations for half a day. During the six years of measurement the kinetic curves show that

$\Phi_{PSII}$ in saline medium is always higher than the control except during 2014. The water conditions alone do not explain this difference between the years because the water deficits between the years 2014 and 2015 were roughly the same (138 and 139). It seems that other environmental factors contributed to buffer $\Phi_{PSII}$ variations in 2014. Nevertheless, the adaptive capacity of an invasive plant in salt-meadows, *Spartina patens* (Aiton) Muhl. was related to maintaining a high level of $\Phi_{PSII}$ despite the increase in salinity (Duarte et al., 2015). We can therefore consider that maintaining a high level of $\Phi_{PSII}$ of *F. angustifolia* in a salty environment is an adaptive trait.

In order to highlight the mechanisms involved in the regulation of $\Phi_{PSII}$, a multivariate analysis was conducted. PCA analysis revealed that the main explanatory variables were the fraction of absorbed energy that is dissipated thermally by the ΔpH- and the xanthophyll cycle-dependent quenching in PSII ($\Phi_{NPQ}$), qP and Fd/Fs ratio. The one-way ANCOVA performed on $\Phi_{NPQ}$ confirms significant differences between salty and control environments (Fig. 6) with the exception of the years 2014 and 2015. In particular, the high yields of $\Phi_{PSII}$ in saline environments may be explained by a better efficiency in the conversion of the light energy absorbed into reducing power since $\Phi_{NPQ}$ is low. However, in another survey it has been reported that low $\Phi_{NPQ}$ values indicate a lower photoprotection capacity in the salt marsh environmental condition (Arena et al., 2013). Photoinhibition mitigation was checked through the analysis of carotenoid contents but this did not show any site effect suggesting the need of further studies on individual xanthophylls characterization. Because no difference was found in leaves $Na^+$ content it is likely that ash individuals in the meadow have evolved specific mechanisms of salt retention/exclusion at the root level. Indeed, several reports have shown that glycophytes may adapt to salt stress by sequestering sodium ions in their root compartment (Assaha et al., 2017; Chen et al., 2018). Among the mechanisms involved, the apoplastic barrier through the casparian strip seems to play a critical role in controlling $Na^+$ uptake and transport into the shoots. This is supported by the identification of suberin-forming key genes as *SbKCS11* (Chen et al., 2018).

Given the exclusion of salt from foliar cytoplasm, it appears that the major adaptive constraint of ash is water availability since the water deficit follows the growth pattern. Precisely, the greater the water deficit is the more saline concentration increases thus making the water less accessible to glycophytes. The concomitant fluorescence and gas exchange measurements carried out in 2009 showed that the net assimilation of $CO_2$ was the same regardless of the difference of salinity between the two sites. It is likely that the higher values of $\Phi_{PSII}$ obtained

in saline areas corresponds to a supplementary energy demand to sustain growth and adaptation to water/salt stress. When considering the radial growth of *F. angustifolia* that declines since 2011, both ATP and the anabolic coenzyme NADPH from photosynthesis light-dependent reactions and the carbon assimilated are rather allocated to defencse processes. The tradeoffs between lignin biosynthesis and defense still remain challenging although jasmonic acid and phytochrome B signalling pathway was identified as a hub that coordinate plants growth and defense (Xie et al., 2018). Interestingly, differential analysis of genes expressed in response to salt stress in *Fraxinus velutina* showed that the up-regulated genes mainly concerned those of the biosynthetic pathway of alkaloids which are also known as defense components (Yan et al., 2019).

## 5. Conclusion

In conclusion, this work, carried out for 6 years between 2007 and 2016, highlighted some of the adaptive mechanisms of a glycophyte in salt meadows environmental condition. Since 2011, a decline has been observed in the production of ash biomass in saline environments. This decline seems mainly related to recurrent water deficit. In the perspective of the climate change announced in the Mediterranean region, one could expect an extinction of ash in salt meadows. *F. angustifolia* resistance was shown by the establishment of an efficient photochemical yield both by a reduction of the fraction of the absorbed radiation which is dissipated as heat and also by increasing the concentration of chlorophyll a. However, non-native salt marsh species with a high tolerance to salinity and drought will be least affected by the sea-level increase and drought associated to global change. Further studies are needed to establish the metabolic network involved in the adaptive strategies of glycophytes in saline environments.

**Acknowledgements:** The authors gratefully acknowledge Mrs Christine Desouches and Météo-France for providing the meteorological data. Dr Julien Ruffault is also acknowledged for graph fitting with R software.

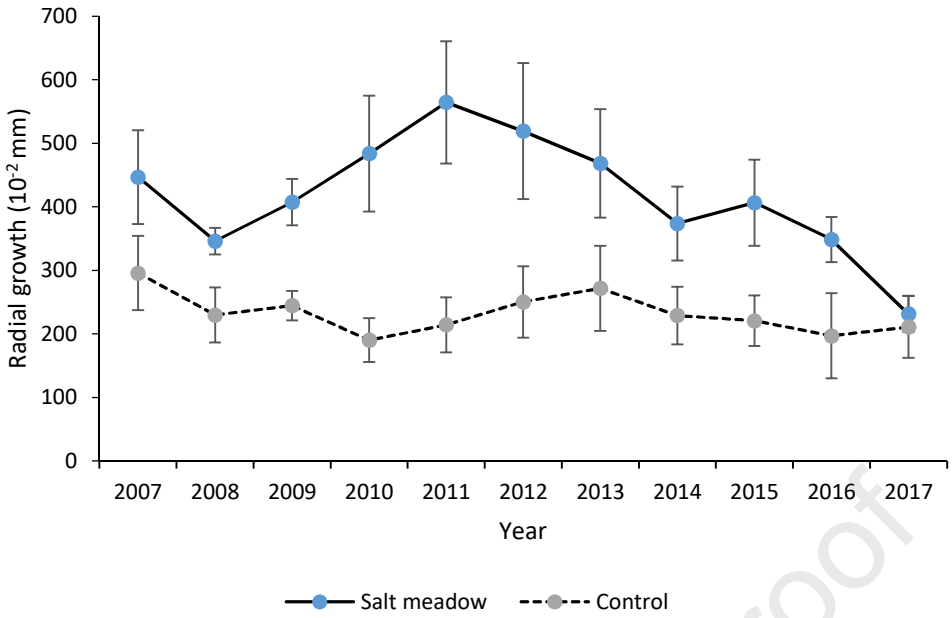


446

447 Fig. 1: Annual radial growth of *Fraxinus angustifolia* from trees of salt meadow ecotone and
448 the control riparian forest from 2007-2017. *n*=6, means ± SE)

449

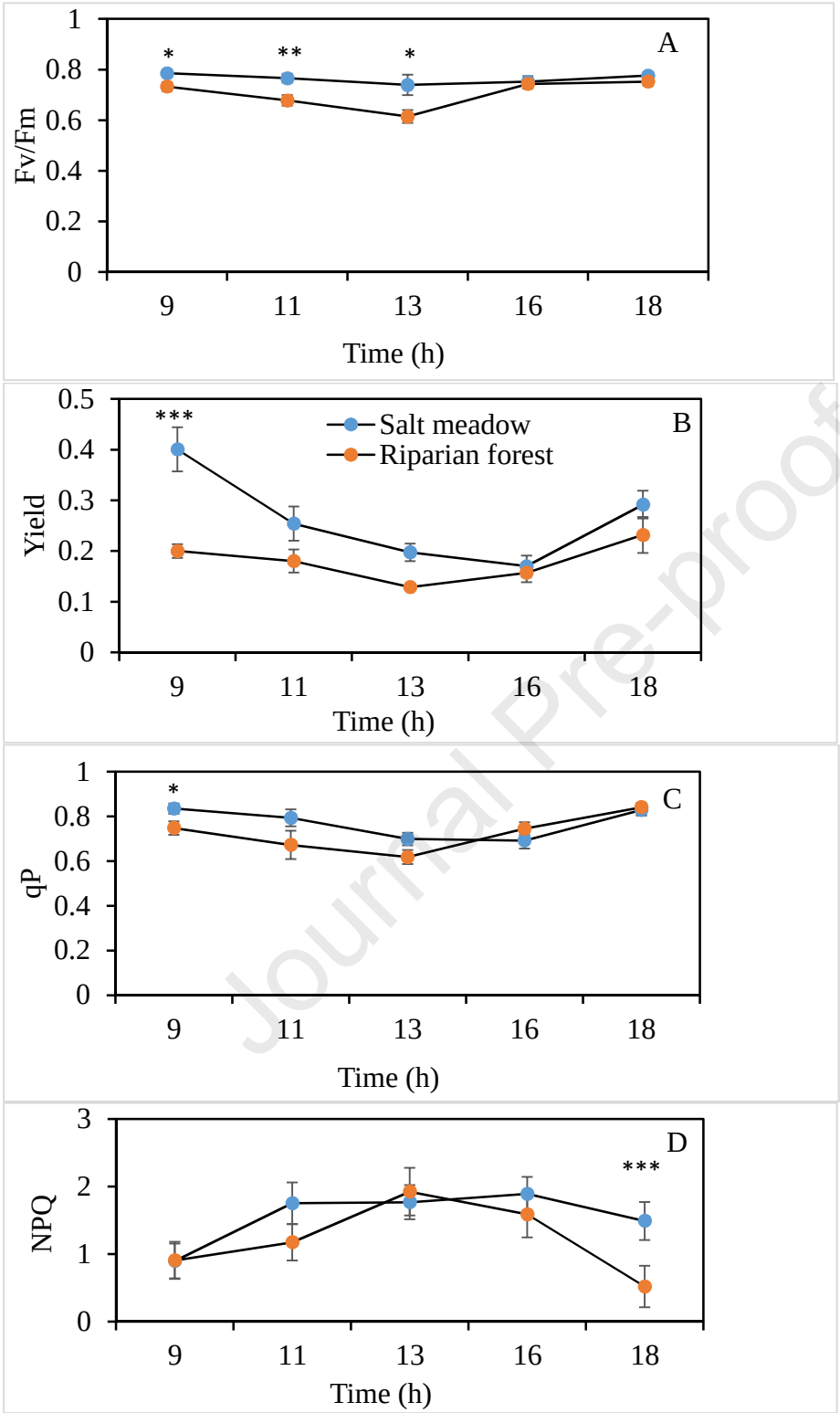


Fig. 2 : Diurnal course of summer fluorescence measurements from *Fraxinus angustifolia* in salt meadow and riparian forest sites: The ratio Fv/Fm (A), the actual quenching yield (B), the photochemical quenching qP (C), and the Non-Photochemical Quenching NPQ (D). A student test was applied to compare the sites at each interval of time.*- $P<0.05$, **- $P<0.01$, ***- $P<0.001$. $n = 6$, means ± SE

458

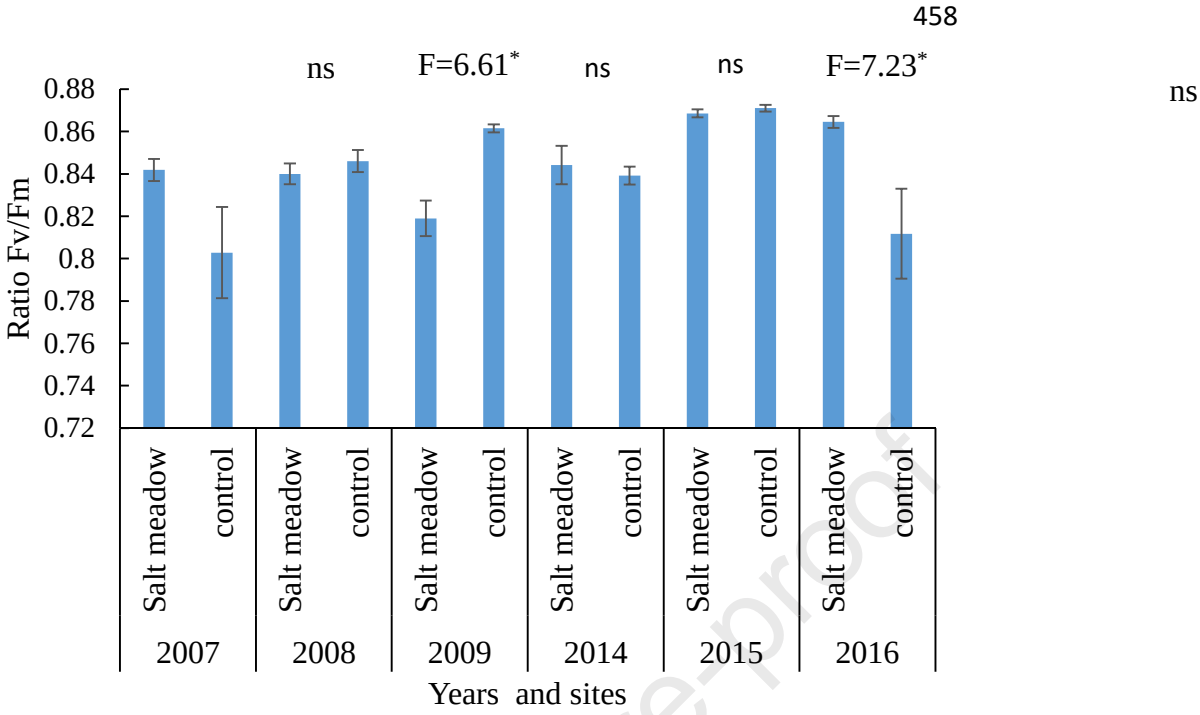


470

471 Fig.3: Predawn Fv/Fm ratio of *Fraxinus angustifolia* from salt meadow and the control
472 riparian forest between 2007 and 2016. The test was performed year by year (one-way-
473 ANOVA, *- $p<0.05$, ns- not significant, $n=18$, means ± SD).

474

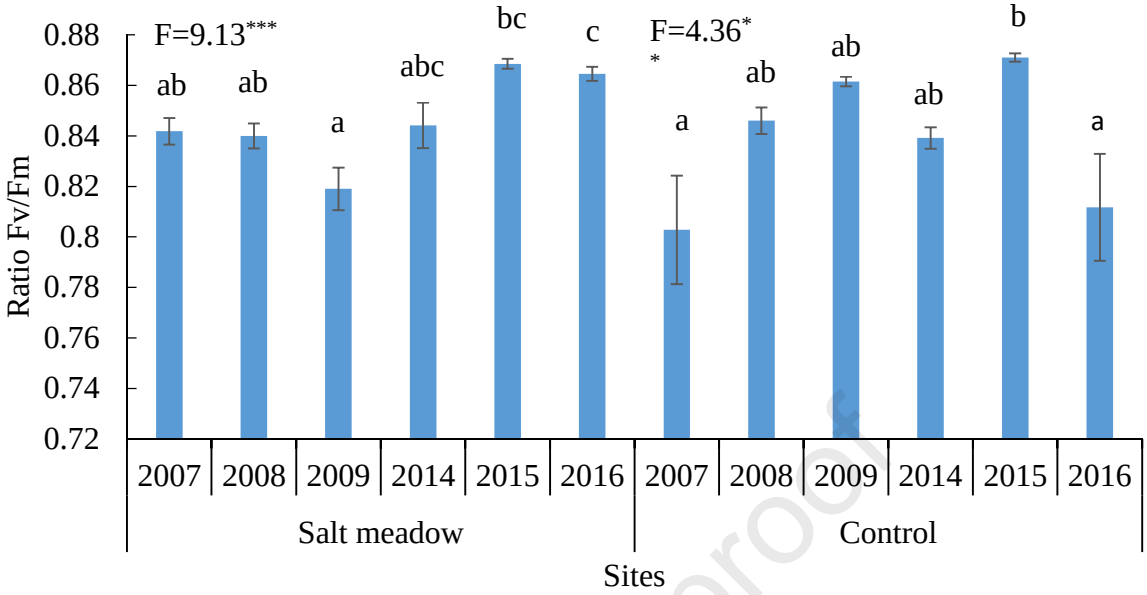


476

477 Fig. 4: Predawn Fv/Fm ratio of *Fraxinus angustifolia* from salt meadow and the control
478 riparian forest between 2007 and 2016. The test was performed site by site (one-way-
479 ANOVA, **-$p$<0.001, ns- not significant, $n$=18, means ± SD).

480

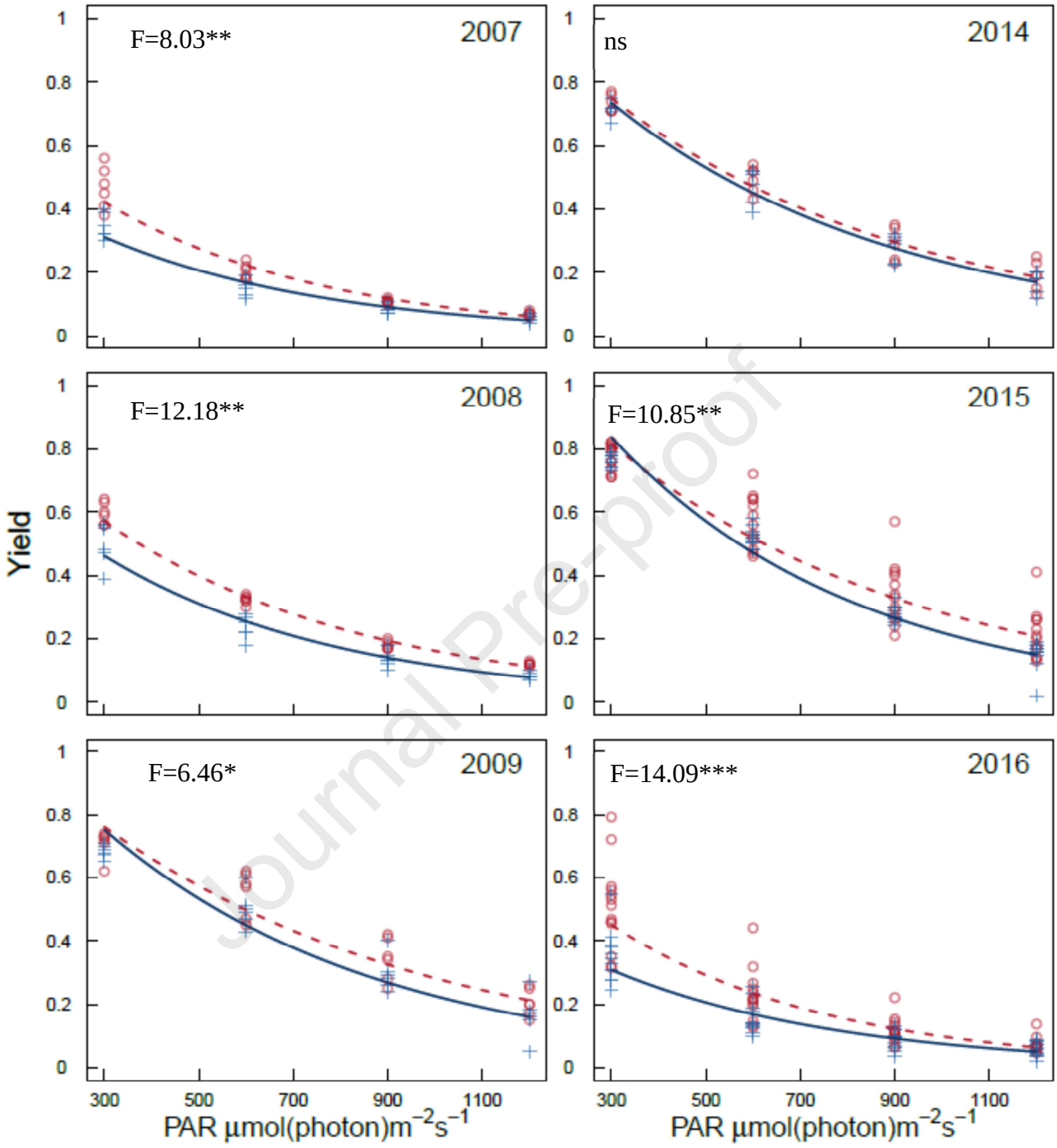


Fig. 5: Light response of PSII actual quantum yield of *Fraxinus angustifolia* in salt meadow (red dotted line) and riparian forest sites (blue line). one-way-ANCOVA. *- $P<0.05$, ** - $P<0.01$, ***- $P<0.001$.

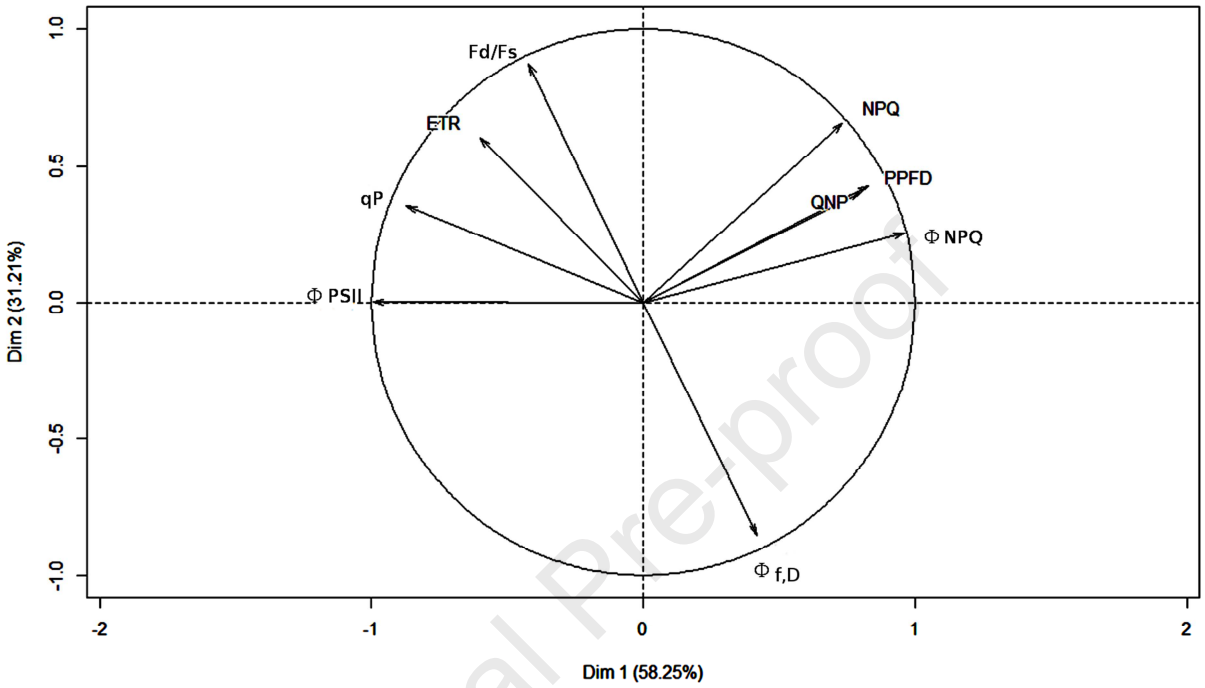


Fig. 6: Principal Component Analysis (PCA) of the fluorescence variables map on axes 1 and 2 plus the correlation circle: The photochemical efficiency in the light adapted state of photosystem II ($\Phi_{PSII}$), the non-photochemical quenching coefficient (NPQ), the photochemical quenching coefficient (qP), the regulated ΔpH and/or xanthophyll-dependent non-photochemical dissipation processes ($\Phi_{NPQ}$), the constitutive non-photochemical fluorescence and energy dissipation ($\Phi_{f,D}$), the ratio Fd/Fs, the Photosynthetic Photon Flux Density (PPFD), the Electron Transport Rate (ETR) and the alternative non-photochemical quenching coefficient, QNP.

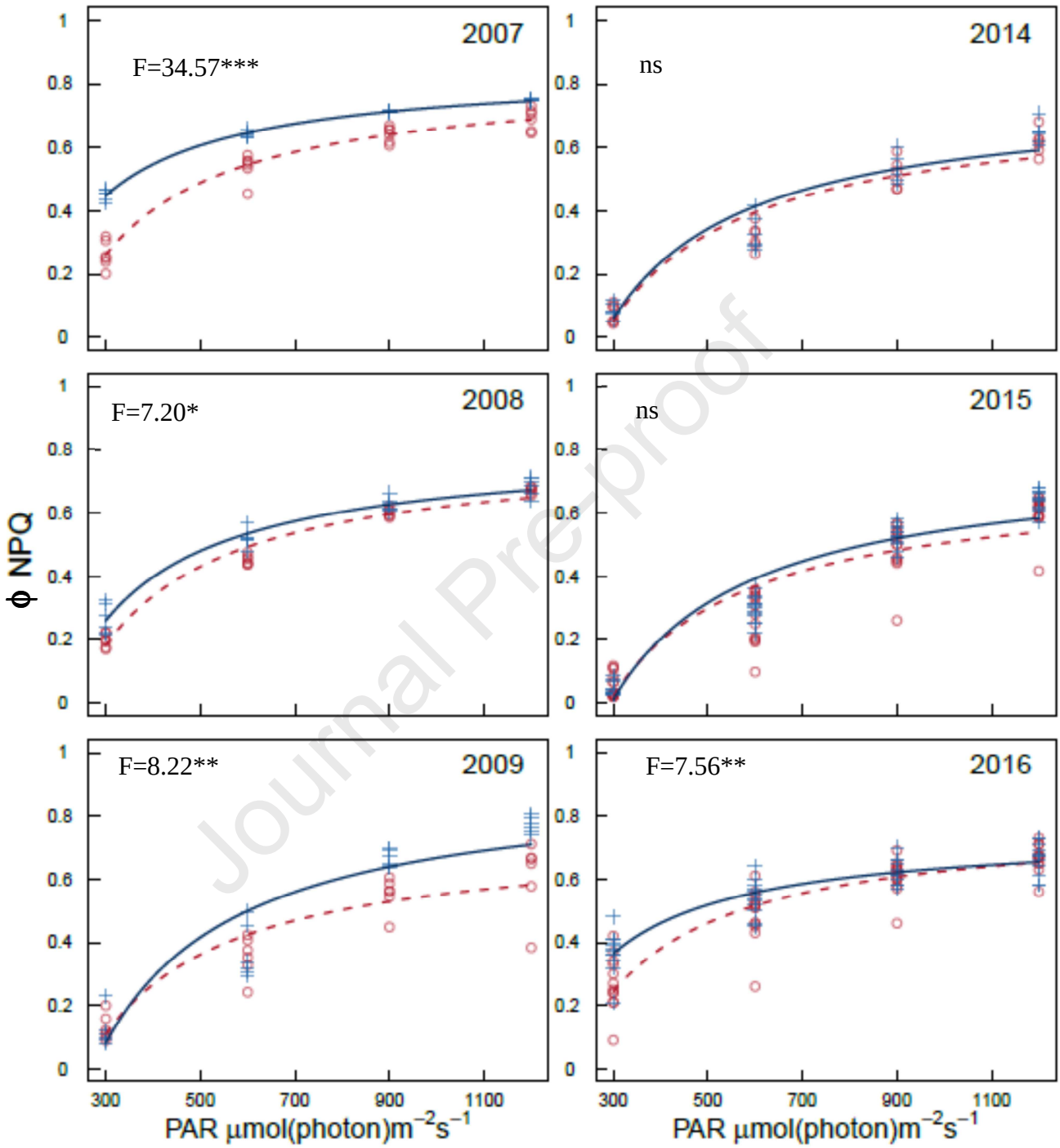


Fig.7: Light response of PSII Non-Photochemical Quenching yield of *Fraxinus angustifolia* in salt meadow (red dotted line) and riparian forest sites (blue line). one-way-ANCOVA.

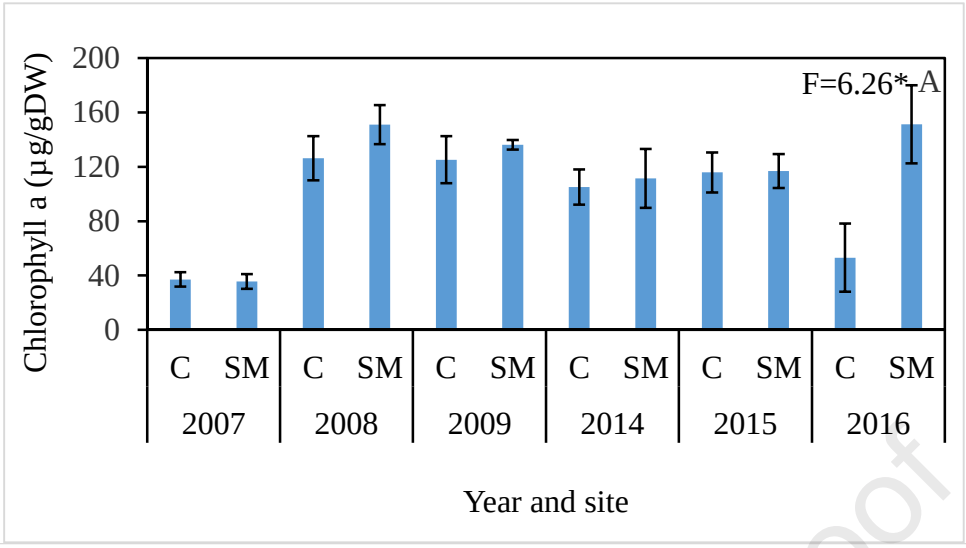


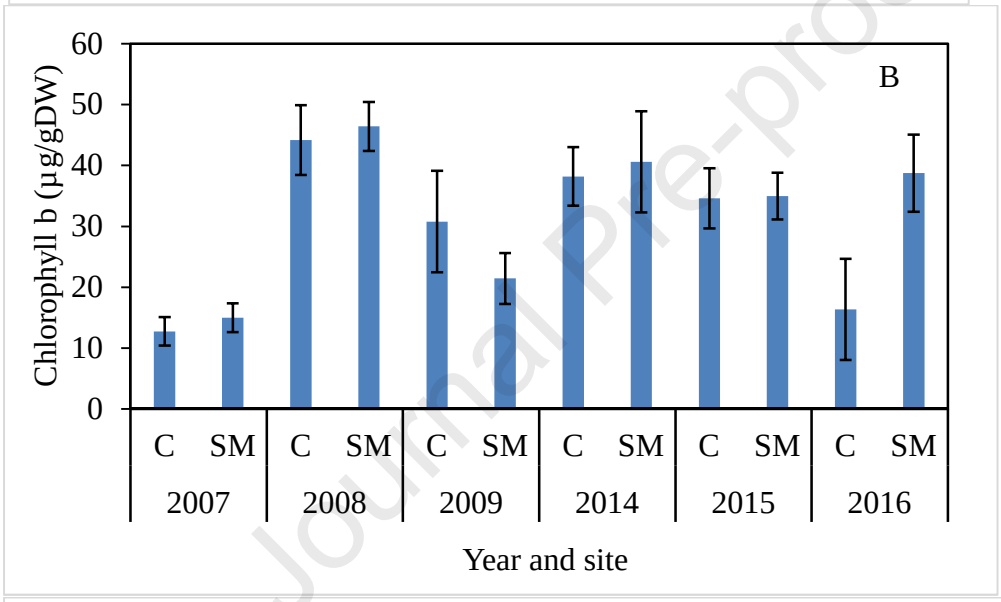


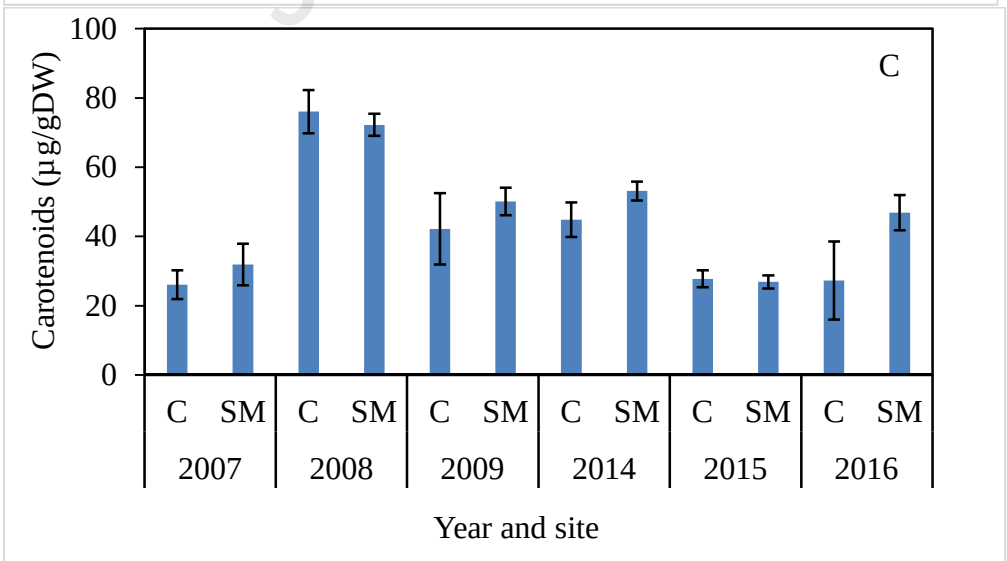


509 Fig. 8: Interannual variations of photosynthetic pigments from *Fraxinus angustifolia* in salt
510 meadow (SM) and riparian forest (C) stands (*n*=5 means ± SE). A; Chlorophyll a content.

511 Sites are compared year-by-year, one-way ANOVA, * - $P<0.05$. B; Chlorophyll b content (no
512 site effect, $P>0.05$). C; Carotenoids content (no site effect, $P>0.05$).

| Sampling date | Air temperature (°C) | Precipitations (P ; mm) | Potential evapotranspiration (PET ; mm) | Water deficit (mm) |
|---|---|---|---|---|
| Summer 2007 | 23.53±1.10 | 36.8 | 635.7 | -598.9 |
| Summer 2008 | 23.87±2.28 | 27.6 | 649.1 | -621.5 |
| Summer 2009 | 24.88±1.79 | 109.8 | 691.3 | -581.5 |
| Summer 2011 | 22.86±1.81 | 191.2 | 609.6 | -418.4 |
| Summer 2014 | 23.53±0.99 | 138.5 | 646.0 | -507.5 |
| Summer 2015 | 25.14±1.66 | 139.0 | 675.8 | -536.8 |
| Summer 2016 | 24.42±1.80 | 10.0 | 669.8 | -659.8 |

513

514 Table 1: Annual variations and climatic variables of Marignane (France) station close to the
515 study area. Climatic data for 3 months in summer before each sampling date. Average air
516 temperature (± SD) of decadal data in each year (n = 9). Cumulative values (P and PET) are
517 calculated from daily data for each summer (n = 90). Water deficit: P-PET. Air temperature
518 test: One-way-ANOVA, $F$=2.12, $P$=0.065).

| | Predawn leaf water potential (MPa) | Leaf cation $Na^+$ content (g/g of ash) | Soil $Na^+$ content (g/l of soil solution) |
|---|---|---|---|
| Salt meadow | -4.61 (0.24) | 0.74 (0.23) | 20.74 (8.50) |
| Riparian forest | -4.13 (0.21) | 0.76 (0.23) | 1.63 (0.09) |

519

520 Table 2: Predawn leaf water potential, leaf and soil $Na^+$ contents from Salt meadow and
521 riparian forest of *Fraxinus angustifolia* in august 2007.

522

| Site | Net photosynthesis (A; µmol $CO_2$. $m^{-2}.s^{-1}$) | $\Phi_{PSII}$ | Fv'/Fm' | qP | Ci (µmol $CO_2$ $mol^{-1}$) |
|---|---|---|---|---|---|
| Control | 2.93 (0.53) | 0.24 (0.01) | 0.44 (0.01) | 0.54 (0.03) | 261.70 (25.82) |
| Salt meadow | 3.17 (0.84) | 0.24 (0.03) | 0.42 (0.01) | 0.55 (0.06) | 273.98 (26.58) |

524

525 Table 3: Gas exchange and fluorescence measurements from leaves of *Fraxinus angustifolia*
526 in salt meadow and riparian forest stands. (*n*=12, means ±SD).

527

528

## References


Acosta-Motos, J.R., Ortuño, M.F., Bernal-Vicente, A., Diaz-Vivancos, P., Sanchez-Blanco, M.J., Hernandez, J.A., 2017. Plant Responses to Salt Stress: Adaptive Mechanisms. Agronomy 7, 18. https://doi.org/10.3390/agronomy7010018

Arena, C., De Micco, V., De Maio, A., Mistretta, C., Aronne, G., Vitale, L., 2013. Winter and summer leaves of Cistus incanus: differences in leaf morphofunctional traits, photosynthetic energy partitioning, and poly(ADP-ribose) polymerase (PARP) activity. Botany 91, 805–813. https://doi.org/10.1139/cjb-2013-0121

Assaha, D.V.M., Mekawy, A.M.M., Liu, L., Noori, M.S., Kokulan, K.S., Ueda, A., Nagaoka, T., Saneoka, H., 2017. Na+ Retention in the Root is a Key Adaptive Mechanism to Low and High Salinity in the Glycophyte, Talinum paniculatum (Jacq.) Gaertn. (Portulacaceae). J Agro Crop Sci 203, 56–67. https://doi.org/10.1111/jac.12184

Bang, J.H., Bae, M.-J., Lee, E.J., 2018. Plant distribution along an elevational gradient in a macrotidal salt marsh on the west coast of Korea. Aquatic Botany 147, 52–60. https://doi.org/10.1016/j.aquabot.2018.03.005

Bilger, W., Björkman, O., 1990. Role of the xanthophyll cycle in photoprotection elucidated by measurements of light-induced absorbance changes, fluorescence and photosynthesis in leaves of Hedera canariensis. Photosynth Res 25, 173–185. https://doi.org/10.1007/BF00033159

Björkman, O., Demmig, B., 1987. Photon yield of O2 evolution and chlorophyll fluorescence characteristics at 77 K among vascular plants of diverse origins. Planta 170, 489–504. https://doi.org/10.1007/BF00402983

Boughalleb, F., Denden, M., Tiba, B.B., 2009. Photosystem II photochemistry and physiological parameters of three fodder shrubs, Nitraria retusa, Atriplex halimus and Medicago arborea under salt stress. Acta Physiol Plant 31, 463–476. https://doi.org/10.1007/s11738-008-0254-3

Chai, W.-W., Wang, W.-Y., Ma, Q., Yin, H.-J., Hepworth, S.R., Wang, S.-M., 2019. Comparative transcriptome analysis reveals unique genetic adaptations conferring salt tolerance in a xerohalophyte. Funct. Plant Biol. 46, 670–683. https://doi.org/10.1071/FP18295

Chen, M., Yang, Z., Liu, J., Zhu, T., Wei, X., Fan, H., Wang, B., 2018. Adaptation Mechanism of Salt Excluders under Saline Conditions and Its Applications. Int. J. Mol. Sci. 19, 3668. https://doi.org/10.3390/ijms19113668

Dalberto, D.S., Martinazzo, E.G., Bacarin, M.A., 2017. Chlorophyll a fluorescence reveals adaptation strategies in drought stress in Ricinus communis. Braz. J. Bot. 40, 861–870. https://doi.org/10.1007/s40415-017-0412-1

Drvodelic, D., Ugarkovic, D., Orsanic, M., Paulic, V., 2016. The Impact of Drought, Normal Watering and Substrate Saturation on the Morphological and Physiological Condition of Container Seedlings of Narrow-Leaved Ash (Fraxinus angustifolia Vahl). SEEFOR-South-East Eur. For. 7, 135–142. https://doi.org/10.15177/seefor.16-11

Duarte, B., Santos, D., Marques, J.C., Caçador, I., 2015. Ecophysiological constraints of two invasive plant species under a saline gradient: Halophytes versus glycophytes. Estuarine, Coastal and Shelf Science, Coastal systems under change: tuning assessment and management tools 167, 154–165. https://doi.org/10.1016/j.ecss.2015.04.007

Flowers, T.J., Colmer, T.D., 2008. Salinity tolerance in halophytes. New Phytol. 179, 945–963. https://doi.org/10.1111/j.1469-8137.2008.02531.x

Foti, R., Jesus, M. del, Rinaldo, A., Rodriguez-Iturbe, I., 2012. Hydroperiod regime controls the organization of plant species in wetlands. PNAS 109, 19596–19600. https://doi.org/10.1073/pnas.1218056109

Genty, B., Briantais, J.-M., Baker, N.R., 1989. The relationship between the quantum yield of photosynthetic electron transport and quenching of chlorophyll fluorescence. Biochimica et Biophysica Acta (BBA) - General Subjects 990, 87–92. https://doi.org/10.1016/S0304-4165(89)80016-9

Gharbi, E., Martínez, J.-P., Benahmed, H., Lepoint, G., Vanpee, B., Quinet, M., Lutts, S., 2017. Inhibition of ethylene synthesis reduces salt-tolerance in tomato wild relative species Solanum chilense. Journal of Plant Physiology 210, 24–37. https://doi.org/10.1016/j.jplph.2016.12.001

Hasegawa, P.M., 2013. Sodium (Na+) homeostasis and salt tolerance of plants. Environ. Exp. Bot. 92, 19–31. https://doi.org/10.1016/j.envexpbot.2013.03.001

Hendrickson, L., Förster, B., Pogson, B.J., Chow, W.S., 2005. A simple chlorophyll fluorescence parameter that correlates with the rate coefficient of photoinactivation of Photosystem II. Photosynth Res 84, 43–49. https://doi.org/10.1007/s11120-004-6430-4

Holmes, R.L., 1983. Computer-Assisted Quality Control in Tree-Ring Dating and Measurement.

Hu, J., Peng, J., Zhou, Y., Xu, D., Zhao, R., Jiang, Q., Fu, T., Wang, F., Shi, Z., 2019. Quantitative Estimation of Soil Salinity Using UAV-Borne Hyperspectral and Satellite Multispectral Images. Remote Sens. 11, 736. https://doi.org/10.3390/rs11070736

James, M.L., Zedler, J.B., 2000. Dynamics of Wetland and Upland Subshrubs at the Salt Marsh-Coastal Sage Scrub Ecotone. The American Midland Naturalist 143, 298–311.

Lichtenthaler, H.K., Buschmann, C., Knapp, M., 2005. How to correctly determine the different chlorophyll fluorescence parameters and the chlorophyll fluorescence decrease ratio RFd of leaves with the PAM fluorometer. Photosynthetica 43, 379–393. https://doi.org/10.1007/s11099-005-0062-6

Lichtenthaler, H.K., Wellburn, A.R., 1983. Determinations of total carotenoids and chlorophylls a and b of leaf extracts in different solvents. Biochem Soc Trans 11, 591–592. https://doi.org/10.1042/bst0110591

Manaa, A., Goussi, R., Derbali, W., Cantamessa, S., Abdelly, C., Barbato, R., 2019. Salinity tolerance of quinoa (Chenopodium quinoa Willd) as assessed by chloroplast ultrastructure and photosynthetic performance. Environmental and Experimental Botany 162, 103–114. https://doi.org/10.1016/j.envexpbot.2019.02.012

Masondo, N.A., Aremu, A.O., Kulkarni, M.G., Petřík, I., Plačková, L., Šubrtová, M., Novák, O., Grúz, J., Doležal, K., Strnad, M., Finnie, J.F., Van Staden, J., 2019. How Do Different Watering Regimes Affect the Growth, Chlorophyll Fluorescence, Phytohormone, and Phenolic Acid Content of Greenhouse-Grown Ceratotheca triloba? J Plant Growth Regul 38, 385–399. https://doi.org/10.1007/s00344-018-9848-1

Maxwell, K., Johnson, G.N., 2000. Chlorophyll fluorescence—a practical guide. J Exp Bot 51, 659–668. https://doi.org/10.1093/jexbot/51.345.659

Pennings, S.C., Grant, M.-B., Bertness, M.D., 2005. Plant zonation in low-latitude salt marshes: disentangling the roles of flooding, salinity and competition. Journal of Ecology 93, 159–167. https://doi.org/10.1111/j.1365-2745.2004.00959.x

Scholander, P.F., Bradstreet, E.D., Hemmingsen, E.A., Hammel, H.T., 1965. Sap Pressure in Vascular Plants: Negative hydrostatic pressure can be measured in plants. Science 148, 339–346. https://doi.org/10.1126/science.148.3668.339

Schreiber, U., Schliwa, U., Bilger, W., 1986. Continuous recording of photochemical and non-photochemical chlorophyll fluorescence quenching with a new type of modulation fluorometer. Photosyn. Res. 10, 51–62. https://doi.org/10.1007/BF00024185

Shoukat, E., Abideen, Z., Ahmed, M.Z., Gulzar, S., Nielsen, B.L., 2019. Changes in growth and photosynthesis linked with intensity and duration of salinity in Phragmites karka.

Environmental and Experimental Botany 162, 504–514. https://doi.org/10.1016/j.envexpbot.2019.03.024

Silvestri, S., Defina, A., Marani, M., 2005. Tidal regime, salinity and salt marsh plant zonation. Estuarine, Coastal and Shelf Science 62, 119–130. https://doi.org/10.1016/j.ecss.2004.08.010

Thorne, K.M., Takekawa, J.Y., Elliott-Fisk, D.L., 2012. Ecological Effects of Climate Change on Salt Marsh Wildlife: A Case Study from a Highly Urbanized Estuary. Journal of Coastal Research 1477–1487. https://doi.org/10.2112/JCOASTRES-D-11-00136.1

Traut, B.H., 2005. The role of coastal ecotones: a case study of the salt marsh/upland transition zone in California. Journal of Ecology 93, 279–290. https://doi.org/10.1111/j.1365-2745.2005.00969.x

Tsai, Y.-C., Chen, K.-C., Cheng, T.-S., Lee, C., Lin, S.-H., Tung, C.-W., 2019. Chlorophyll fluorescence analysis in diverse rice varieties reveals the positive correlation between the seedlings salt tolerance and photosynthetic efficiency. BMC Plant Biol. 19, 403. https://doi.org/10.1186/s12870-019-1983-8

Vaz, M., Coelho, R., Rato, A., Samara-Lima, R., Silva, L.L., Campostrini, E., Mota, J.B., 2016. Adaptive strategies of two Mediterranean grapevines varieties (Aragonez syn. Tempranillo and Trincadeira) face drought: physiological and structural responses. Theor. Exp. Plant Physiol. 28, 205–220. https://doi.org/10.1007/s40626-016-0074-6

Veldkornet, D.A., Adams, J.B., Potts, A.J., 2015. Where do you draw the line? Determining the transition thresholds between estuarine salt marshes and terrestrial vegetation. South African Journal of Botany, Biome Boundaries in South Africa 101, 153–159. https://doi.org/10.1016/j.sajb.2015.05.003

Wang, Y., An, Y., Yu, J., Zhou, Z., He, S., Ru, M., Cui, B., Zhang, Y., Han, R., Liang, Z., 2016. Different responses of photosystem II and antioxidants to drought stress in two contrasting populations of Sour jujube from the Loess Plateau, China. Ecol. Res. 31, 761–775. https://doi.org/10.1007/s11284-016-1384-5

Xie, M., Zhang, J., Tschaplinski, T.J., Tuskan, G.A., Chen, J.-G., Muchero, W., 2018. Regulation of Lignin Biosynthesis and Its Role in Growth-Defense Tradeoffs. Front. Plant Sci. 9, 1427. https://doi.org/10.3389/fpls.2018.01427

Yan, K., Wu, C., Zhang, L., Chen, X., 2015. Contrasting photosynthesis and photoinhibition in tetraploid and its autodiploid honeysuckle (Lonicera japonica Thunb.) under salt stress. Front Plant Sci 6. https://doi.org/10.3389/fpls.2015.00227

Yan, L., Liu, C., Wang, Y., Wang, K., Ren, F., Yao, J., Wu, D., 2019. De novo transcriptome analysis of Fraxinus velutina Torr in response to NaCl stress. Tree Genetics & Genomes 15, 56. https://doi.org/10.1007/s11295-019-1340-y

**Highlights**

Adaptation of a glycophyte as *Fraxinus angustifolia* to salt meadow is determined by:

- An increase of the actual quantum yield of PSII photochemistry
- An increase of chlorophyll a contents
- A lower fraction of absorbed energy that is dissipated thermally by the ΔpH- and the xanthophyll cycle-dependent quenching in PSII ($\Phi_{NPQ}$)
- A higher photochemical quenching (qP) and the ratio Fd/Fs

*Fraxinus angustifolia* in salt meadow is more sensitive to global climate change. Since 2011 a decrease of the tree-rings growth was shown suggesting changes in the specific composition in these areas.

**Declaration of interests**

☒ The authors declare that they have no known competing financial interests or personal relationships that could have appeared to influence the work reported in this paper.

☐The authors declare the following financial interests/personal relationships which may be considered as potential competing interests: